Spinning linearly polarized harmonic generation via polarization shaping

Qingyi Li,[1,2] Yulong Li,[3] Fuming Guo,[1,2] Yujun Yang,[1,2] Mingxing Jin,[1,2] Xi Zhao,[4,*] and Jun Wang[1,2,†]

[1]*Institute of Atomic and Molecular Physics, Jilin University, Changchun 130012, China*

[2]*Jilin Provincial Key Laboratory of Applied Atomic and Molecular Spectroscopy, Jilin University, Changchun 130012, China*

[3]*Beijing Institute of Space Launch Technology, Beijing 100076, China*

[4]*School of Physics and Information Technology, Shaanxi Normal University, Xi'an, Shaanxi 710062, China*

(Received 10 April 2024; accepted 28 May 2024; published 11 June 2024)

Here we theoretically demonstrate the generation of spinning linearly polarized harmonics through the combination of polarization shaping with high-order harmonic generation. Specifically, two orthogonally polarized 800-nm femtosecond pulses with precisely controlled relative peak amplitude were combined to obtain a spinning linearly polarized driving field, with which we show a successful chirality transfer from the driving field to the resultant harmonics through its interaction with isotropic Ar atoms. Systematic investigations of the influence from the polarization rotational speed and the peak amplitude of the driving field were conducted, which reveal that the angular frequency and the harmonic order of spinning linearly polarized harmonics can be manipulated independently. The proposed strategy extends the photon energy of the laser fields with twisted polarization into the extreme ultraviolet region, which paves the way for exploring ultrafast dynamics on the attosecond timescale.

DOI: 10.1103/PhysRevA.109.063112

I. INTRODUCTION

In recent years, laser fields with twisted polarization have been gaining attention. Based on their excellent performance in molecular alignment, orientation, and realization of unidirectional molecular rotation (UDR), polarization-twisted laser fields have played a key role in many areas such as molecular super-rotor generation [1], chiral molecule orientation [2], and gas vortex formation [3]. To date, there are mainly four common methods for generating optical fields with twisted polarization, namely, a pair of cross-polarized and properly delayed laser pulses [4], a chiral train of ultrashort pulses [5], optical centrifuges [6], and polarization-shaped pulses [7]. The production of the so-called polarization-shaped pulses involves the use of two orthogonally polarized and partially overlapped femtosecond laser pulses, which results in a spinning linear polarization by 90° at the overlapping region and remains an overall ultrashort duration. Polarization-shaped pulses have been recognized in inducing UDR and contribute to the study of rotational Doppler effects [8], harmonic generation [9], and optical imaging of spinning molecules [10].

Benefiting from the continuous rotation of polarization and femtosecond pulse duration of UDR, polarization-shaped pulses exhibit more exciting prospects in the detection of ultrafast molecular dynamics with ultrahigh temporal resolution [11–13]. In analogy to the angular streaking technique which uses circularly polarized light to map time to angle [14], the mapping between the direction of the polarization vector and its time evolution in a polarization-shaped pulse can be employed to read the ionization (dissociation) instant of the photoelectron (ion) from its emission direction based on the measured angular distribution, and thus probe the ultrafast molecular dynamics. Based on this strategy, researchers have experimentally clocked the dissociative ionization of hydrogen molecules with a subcycle time resolution driven by a polarization-skewed (PS) femtosecond laser pulse [11,12]. Furthermore, through fine-tuning the time-dependent polarization of the PS field, manipulation of dissociation pathways of hydrogen molecules has been experimentally demonstrated [13].

Despite the success of the above strategy in exploring and manipulating molecular dynamics, there are still significant limitations in the following aspects.

(i) Nonuniform polarization rotation. The polarization direction of the PS field does not evolve linearly with time, causing variations in the cross angle between emission directions of the photoelectron and the ion with respect to changes of molecular orientation. In this situation, to clock different reaction pathways with the highest temporal resolution, only a narrow range of molecular orientation could be selected [11].

(ii) Fixed range of rotation. The overall angle change of the polarization vector in the current PS field is limited to 90°. This typically results in the concentration of momentum distributions only in two relative quadrants and thus imposes higher requirements on the angular resolution to resolve specific dissociation pathways.

(iii) Unsatisfactory temporal resolution. It is claimed that the strategy using the PS field possesses a subcycle time resolution since photoelectrons ionized in adjacent half-cycles end with opposite momenta [12]. Based on this, it is obvious

*Contact author: zhaoxi719@snnu.edu.cn

†Contact author: wangjun86@jlu.edu.cn

that the higher the photon energy of the PS pulses, the shorter the optical cycle duration is, and the higher the corresponding temporal resolution is. Currently, however, the photon energies of the PS pulses used in experiments are primarily in the near-infrared (NIR) range with a half-cycle duration larger than 1 fs, which limits the detection of ultrafast dynamics like double ionization on the attosecond timescale [15].

To address the aforementioned issues, by combining polarization shaping with high-order harmonic generation, here we theoretically demonstrate the production of spinning linearly polarized harmonics (SLPH). These novel harmonics exhibit obvious advantages, including a uniform rotation of linear polarization around the center of the envelope, an adjustable range and angular frequency of polarization rotation, and a tunable harmonic order corresponding to half-cycle duration on the order of several tens of attoseconds. In the following, we first introduce the principle for the generation of a uniformly spinning linearly polarized NIR driving field, and then we numerically solve the time-dependent Schrödinger equation, which describes the interaction between the above driving field and Ar atoms, to obtain the desired SLPH. Furthermore, we show that the angular frequency and the harmonic order of the SLPH can be independently tuned by varying separately the polarization rotational speed and the peak amplitude of the driving field. Finally, we summarize the advantages and potential applications of the SLPH.

II. SPINNING LINEARLY POLARIZED DRIVING FIELD

The kernel for the generation of a driving field with spinning linear polarization is based on the superposition of two orthogonally polarized pulses with successive variation of the relative peak amplitude [7], where the orientation angle α against the X axis of a specific linear polarization is equal to $\arctan(y/x)$, as illustrated in Fig. 1(a). Based on this principle, the generation of a NIR spinning linearly polarized driving field of uniform polarization rotation [Fig. 1(b)] is transformed into a vector decomposition problem, which relies on precise control of the relative peak amplitude cycle by cycle in the two-component fields with a wavelength of 800 nm.

The equation of the spinning linearly polarized driving field $\vec{E}_D$ reads as

$$\vec{E}_D = E_x(t)\cos(\omega t)\vec{e}_x + E_y(t-\tau_R)\cos(\omega t-\varphi_R)\vec{e}_y, \quad (1)$$

where ω is the frequency, τ_R is the relative time delay, and $\varphi_R = \omega\tau_R - \varphi_0$ is the relative phase, with φ_0 being the initial phase difference between the two orthogonally polarized components. Here we set $\tau_R = \varphi_R = 0$ for simplicity. The envelopes E_x and E_y can be expressed as

$$\begin{aligned} E_x(t) &= F_x(t)A_x, \\ E_y(t-\tau_R) &= E_y(t) = F_y(t)A_y, \end{aligned} \quad (2)$$

where F_x and F_y determine the overall Gaussian envelope, and A_x and A_y let the electric field rotate eventually,

$$A_x = \cos(\vec{\alpha}_i),\ A_y = \sin(\vec{\alpha}_i)\ (i = 1 \text{ to } N), \quad (3)$$

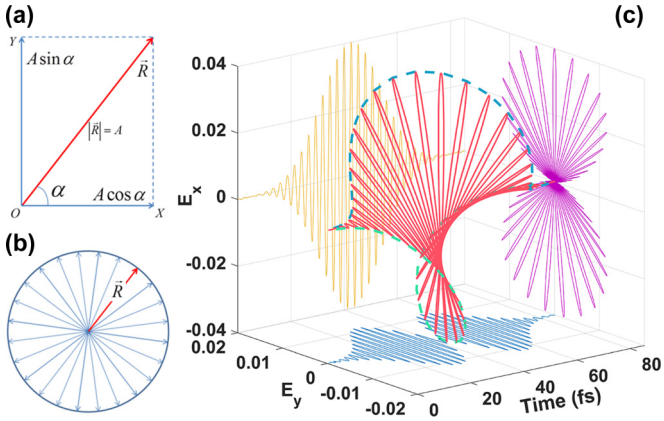

FIG. 1. Schematic illustration of a spinning linearly polarized driving field. (a) Decomposition of a specific polarization vector $\vec{R}$ with a length of A and an orientation angle α against the X axis, where the X-Y plane is perpendicular to the propagation of the driving field along the Z axis. (b) Projection in the X-Y plane of a series of evenly spaced polarization vectors with an equal intersection angle of 15°. (c) Three-dimensional spinning linearly polarized driving field in the counterclockwise direction used in the calculation with 32 optical cycles, wavelength of 800 nm, peak amplitude E_0 of 0.04, and an overall Gaussian envelope.

which control the orientation angle of the ith linear polarization through the angle vector $\vec{\alpha}_i$, and the subscript i ($i = 1$ to N) indicates the sequence of peaks in both of the component fields of N optical cycles. For example, to generate a spinning linearly polarized driving field which totally rotates 360° (2π) through a sequence of linear polarization with the same intersection angle of 15° ($\frac{\pi}{12}$) [Fig. 1(b)], the angle vector $\vec{\alpha}_i$ should be set as $\vec{\alpha}_i = \{\alpha_i \mid \alpha_i = \frac{\pi}{12}, \frac{\pi}{6}, \frac{\pi}{4}, \ldots, 2\pi\}$ with N equal to 24. It should be noted that to conduct multiplication between $F_x(F_y)$ and $A_x(A_y)$ in Eq. (2), a mathematical operation of interpolation on $A_x(A_y)$ is always necessary.

III. THEORETICAL MODEL AND NUMERICAL METHOD

Under the electric dipole approximation and the length gauge, the time-dependent Schrödinger equation of Ar atoms irradiated by the driving field $\vec{E}_D$ is

$$i\frac{\partial}{\partial t}\psi(x,y,t) = \hat{H}(x,y,t)\psi(x,y,t), \quad (4)$$

where the Hamiltonian in Eq. (4) is

$$\hat{H}(x,y,t) = \frac{p_x^2 + p_y^2}{2} + V(x,y) + [xE_x(t) + yE_y(t)]\cos(\omega t). \quad (5)$$

The soft-core Coulomb potential can be expressed as

$$V(x,y) = -\frac{q}{\sqrt{x^2+y^2+a}}, \quad (6)$$

where $q = 1.237$ and $a = 1.0$ is the soft-core parameter corresponding to the ionization potential of an Ar atom. The time-dependent wave function is obtained by the numerical

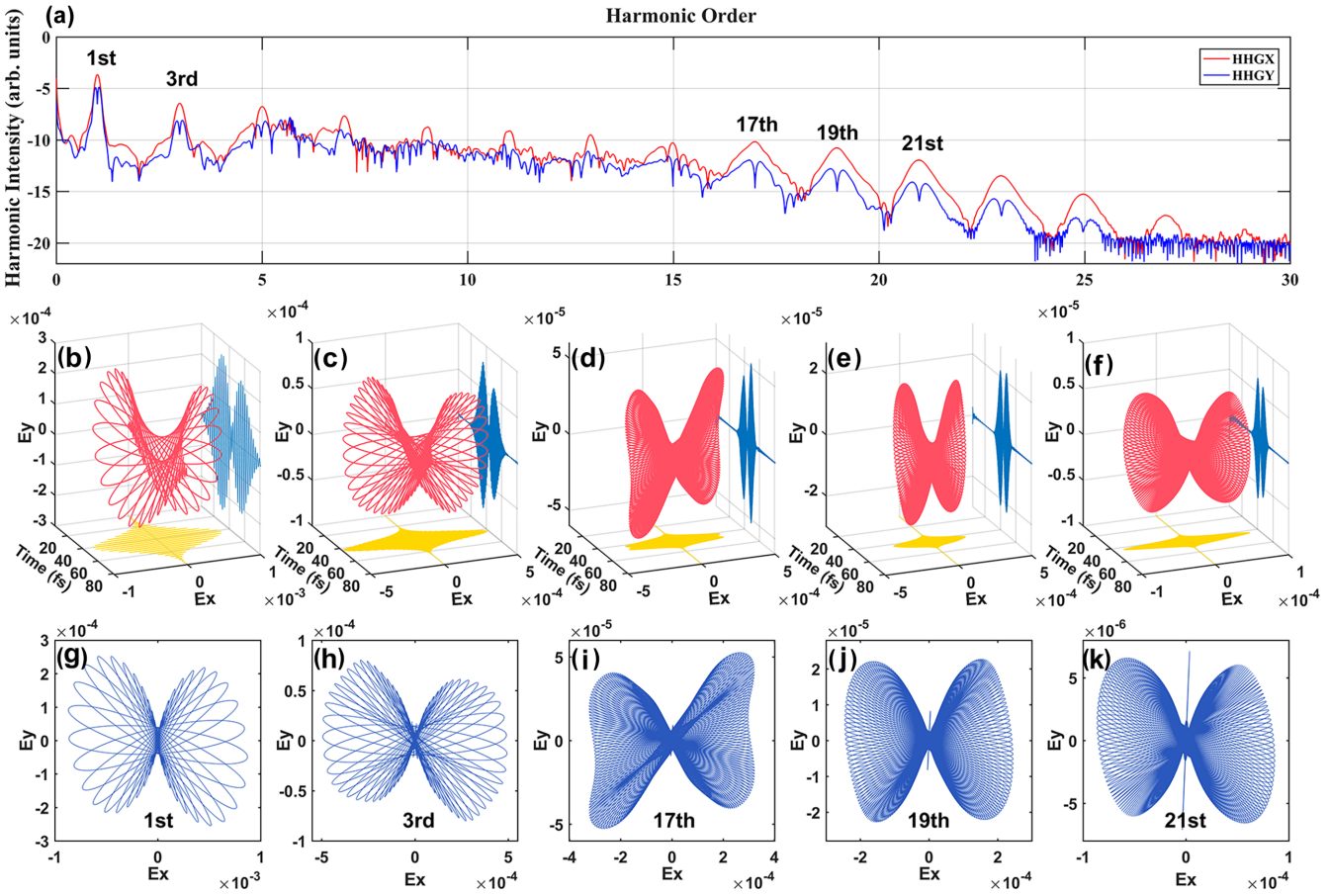

FIG. 2. (a) The X (HHGX) and Y (HHGY) components of the harmonic spectra from Ar atoms irradiated by the spinning linearly polarized driving field shown in Fig. 1(c). The Y axis is plotted in the logarithmic scale. The 1st, 3rd, 17th, 19th, and 21st harmonics are marked to highlight the double-peak structure in HHGY. (b)–(f) The three-dimensional electric field of the corresponding harmonics. (g)–(k) Projections in the X-Y plane of the five selected harmonics, which show obvious twisted polarization and a unique bow-tie shape.

solution of Eq. (4) with the splitting-operator fast-Fourier transform scheme [16–18]. To avoid unphysical reflection of the wave packet from the boundary, the wave function is multiplied by a $\cos^{1/8}$ mask function at each time step. Atomic units are used throughout this paper unless specified otherwise.

IV. RESULTS AND DISCUSSION

In Fig. 2, we provide calculation results of HHG from Ar atoms irradiated by the driving field shown in Fig. 1(c). The 800-nm driving field possesses a Gaussian envelope of 32 optical circles with a full width at half maximum (FWHM) of 8, peak amplitude E_0 of 0.04 (5.61×10^{13} W/cm^2), and a total rotation angle α_{tot} of $\pi(180^\circ)$ in the counterclockwise direction. In Fig. 2(a), the X (HHGX) and Y (HHGY) components of the harmonic spectra are provided in red (upper) and blue (lower), respectively. It is clear that odd harmonics are dominant throughout the harmonic spectra, and HHGX has higher intensities than HHGY, which is consistent with the overall intensity distribution of the driving field's projection in the X-Y plane [purple profile, Fig. 1(c)]. A special feature arises in the harmonic spectra, which manifests itself as a splitting of the odd harmonics in HHGY into a double-peak structure surrounded by the corresponding harmonics in HHGX, and we will show that this new feature is a sign for the appearance of SLPH.

As shown in Fig. 2(a), five odd harmonics are selected and marked by their orders, with which we provide the characteristics of the electric field of SLPH. After an inverse Fourier transform, the corresponding three-dimensional electric field and its projection in the X-Y plane of each of the five selected harmonics are depicted in the middle [panels (b)–(f)] and lower [panels (g)–(k)] rows in Fig. 2, respectively. It is obvious that the electric field of all these selected harmonics exhibit a twisted polarization with X-Y projection of a unique bow-tie shape. Compared with the driving field in Fig. 1(c), apparent depolarization from linear to elliptical polarization happens to the fundamental and the 3rd harmonic, while for each of the other three harmonics near the cutoff (17th, 19th, 21st), more rigorous linear polarization is maintained.

In order to investigate the influence of polarization rotational speed of the driving field on the harmonic spectra and polarization rotation of SLPH, we change the total rotation

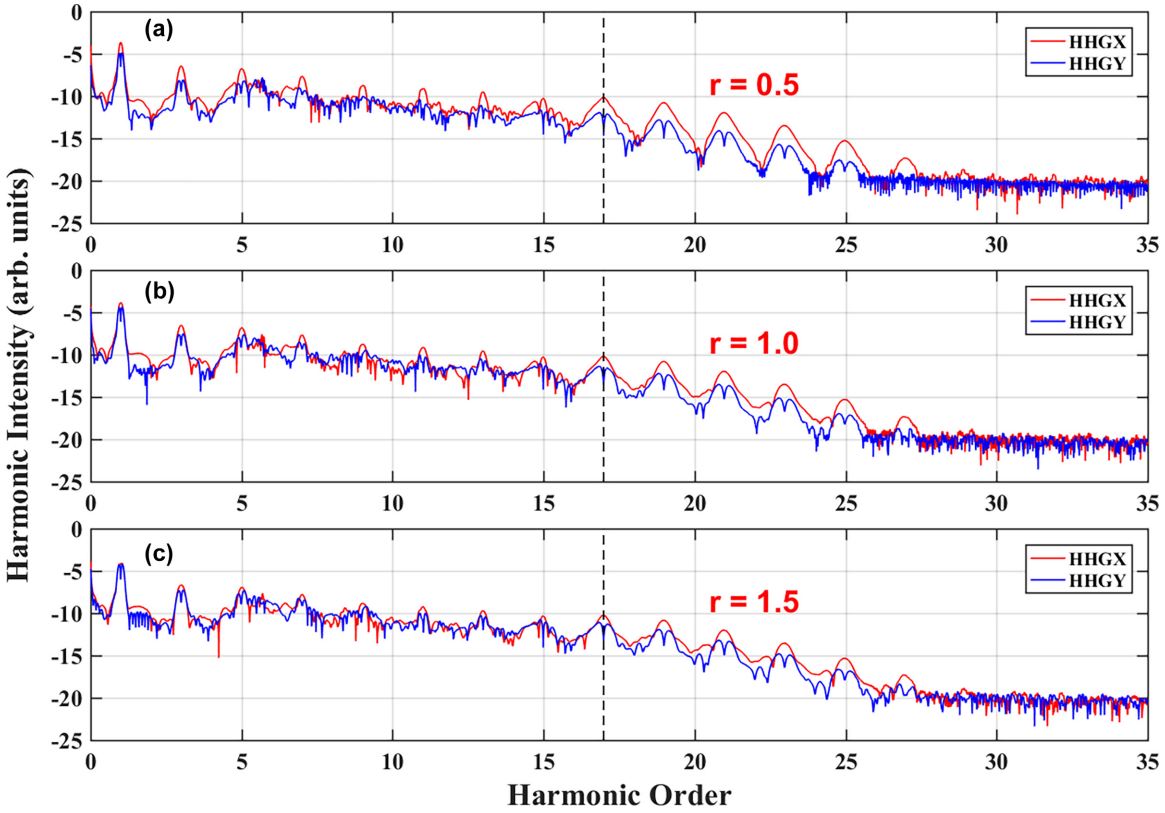

FIG. 3. Harmonic spectra from Ar atoms irradiated by spinning linearly polarized driving fields with distinct parameters r of (a) 0.5, (b) 1.0, and (c) 1.5, respectively. The Y axis is plotted in logarithmic scale. The peak amplitude E_0 is fixed as 0.04.

angle $\alpha_{\rm tot}$ by varying the size of the parameter r, which is defined as $r = \alpha_{\rm tot}/2\pi$ and reflects the number of turns experienced by the linear polarization within N optical cycles. For example, the parameter r equals 0.5 for the driving field in Fig. 1(c) with a total rotation angle $\alpha_{\rm tot}$ of π. By varying the parameter r from 0.5 to 1.0 and 1.5 while fixing N, FWHM, and E_0 unchanged, driving fields with polarization rotational speeds of 2 and 3 times larger are thus obtained, and the corresponding harmonic spectra are shown in Fig. 3. As it is shown, the three harmonic spectra are quite alike generally. The vertical dashed lines mark the cutoff positions, where the 17th harmonic starts to show a spinning linear polarization. With the increase of the polarization rotational speed of the driving field, it is found that the intensity of odd harmonics with double-peak structure in HHGY increases accordingly.

To gain a deeper insight into the influence of parameter r on the polarization rotational speed of SLPH, we trace the orientation angle of linear polarization in the electric field of SLPH as a function of time, and the results are shown in Figs. 4(b)–4(d). In Fig. 4(a), the time evolution of the angle vector $\vec{\alpha}_i$ corresponding to driving fields with different parameters r are provided. As the polarization directions of these driving fields vary linearly with time, their polarization rotational speeds can be readily obtained from the slopes of these mapping curves. For example, the polarization rotational speed of the driving field with parameter $r = 0.5$ is $\sim 2.17^\circ/\text{fs}$, which corresponds to an angular frequency of $\sim 3.79 \times 10^{13}$ rad/s and a frequency of ~ 6.04 THz.

In Figs. 4(b)–4(d), the mappings between the linear polarization direction and its evolution time of the 17th, 19th,

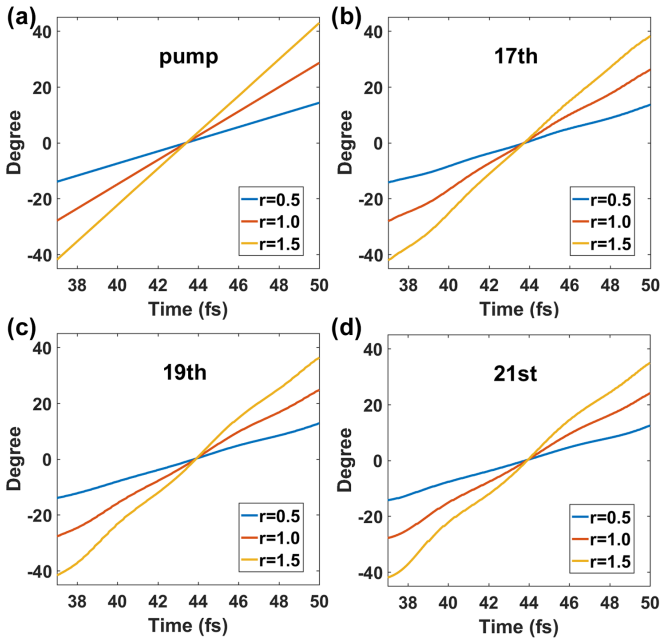

FIG. 4. The mapping between the linear polarization direction and its evolution time of (a) the driving fields and the corresponding (b) 17th, (c) 19th, and (d) 21st spinning linearly polarized harmonics with parameters r of 0.5, 1.0, and 1.5, respectively.

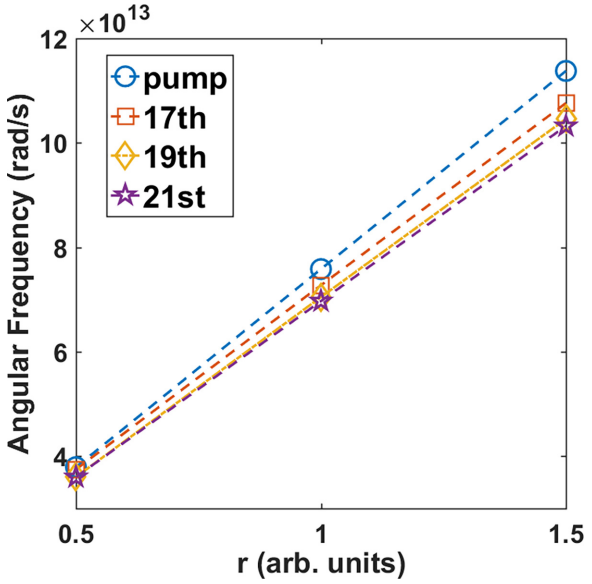

FIG. 5. The average angular frequency of the driving fields (blue circles) and the 17th (orange squares), 19th (yellow diamonds), and 21st (purple stars) SLPHs with an increase of parameter r from 0.5 to 1.0 and 1.5. The peak amplitude E_0 is fixed as 0.04.

and 21st SLPH are shown, respectively. The positive slopes of the mapping curves in Figs. 4(b)–4(d) identical to those in Fig. 4(a) reveal that the linear polarization of these SLPHs also rotates in the counterclockwise direction. This correlation provides chirality control of the SLPH by directly adjusting the rotation direction of the driving field. Around the center of the envelope from 37 to 50 fs, the mapping curves of the SLPH remain almost linear despite slight perturbations with larger parameter r. As the parameter r increases, the slope is enlarged accordingly, which reflects the acceleration of the polarization rotation of the SLPH. These observations clearly demonstrate that the chirality and the rotational behavior can be successfully transferred from the spinning linearly polarized driving field to the SLPH, and this is further quantitatively clarified by the correlation between the average angular frequency of the SLPH and that of the corresponding driving fields, which is shown in Fig. 5.

Besides the control of the polarization rotational speed of the SLPH via parameter r, the manipulation of the harmonic photon energy through turning the harmonic order of the SLPH is equally significant. As mentioned above, SLPH occurs around the cutoff position $I_P + 3.17U_P$ of the corresponding harmonic spectra, where the ponderomotive energy $U_P = E_0^2/4\omega^2$, with E_0 being the peak amplitude and ω the laser frequency of the driving field. This discovery suggests a strategy for turning the order of SLPH by simply varying the amplitude E_0. To verify the feasibility of this strategy, in Figs. 6(a)–6(c) we provide the harmonic spectra from Ar atoms irradiated by spinning linearly polarized driving fields

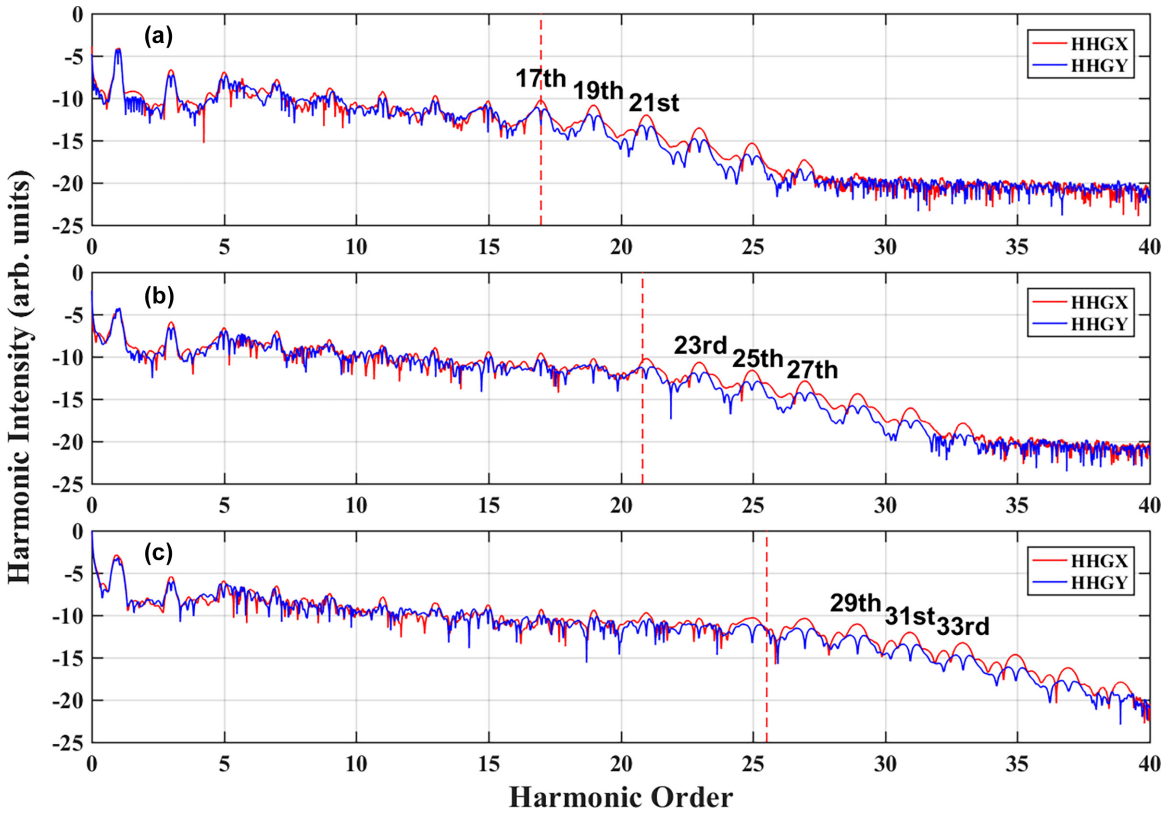

FIG. 6. Harmonic spectra from Ar atoms irradiated by spinning linearly polarized driving fields with distinct peak amplitudes E_0 of (a) 0.04, (b) 0.05, and (c) 0.06, respectively. The parameter r is fixed as 1.5. In each panel, the Y axis is plotted in logarithmic scale, and a red vertical dashed line is shown to highlight the cutoff position.

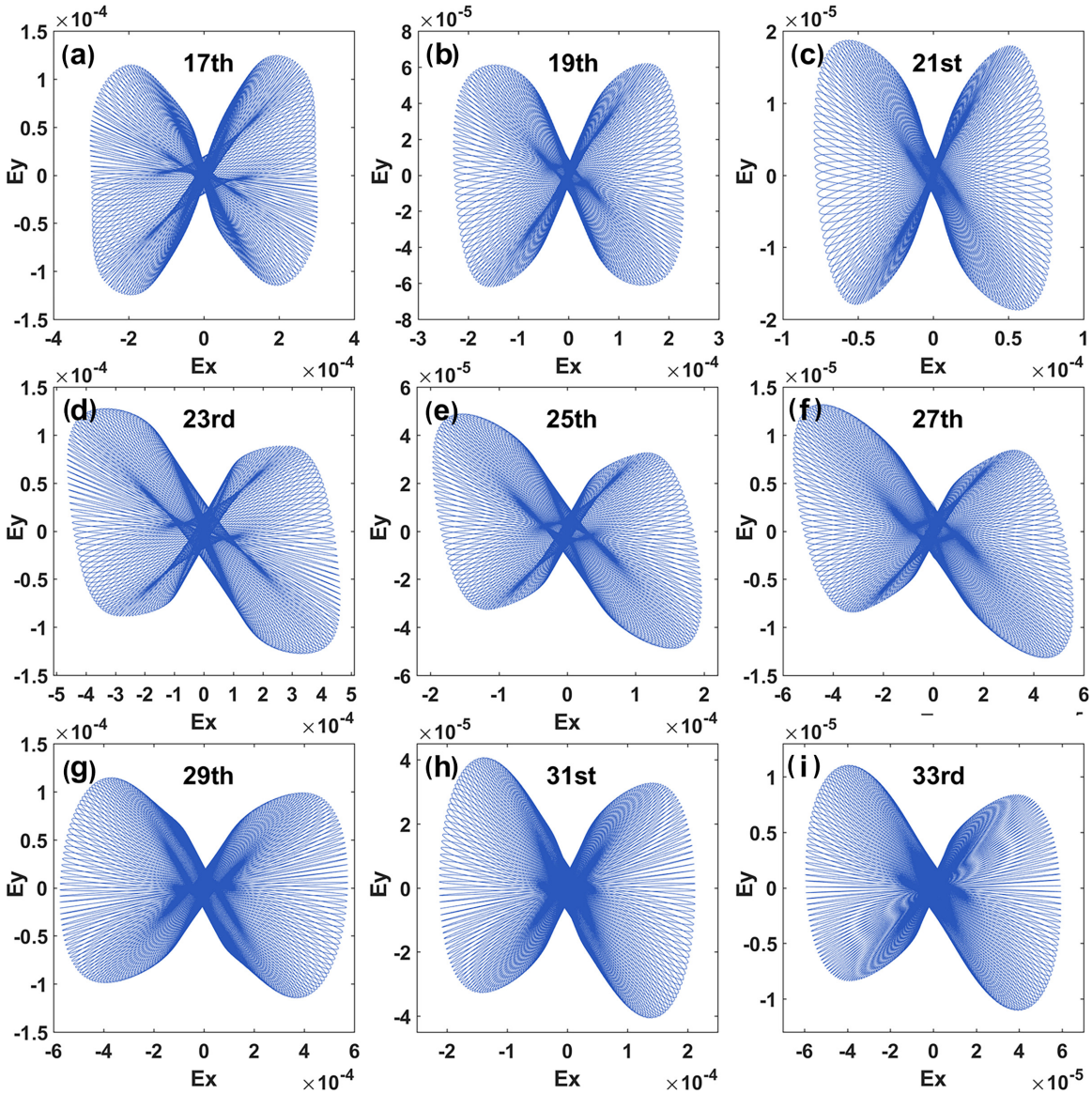

FIG. 7. The projections of the electric field in the X-Y plane of SLPHs with harmonic order from 17th to 33rd. The parameter r is fixed as 1.5, and the peak amplitude E_0 of the driving field increases from 0.04 to 0.05 and 0.06 in each row.

with the parameter $r = 1.5$ and the peak amplitudes E_0 of 0.04, 0.05, and 0.06, respectively. In each panel of Fig. 6, a red vertical dashed line is shown to highlight the cutoff position, which is blue shifted with the increase of E_0. It is obvious that each of the nine marked harmonics with orders from 17th to 33rd around the cutoff exhibits a double-peak structure in HHGY, which has been clarified as a signature of the appearance of SLPH. Furthermore, the projections of the electric field in the X-Y plane and the corresponding angular frequencies of these nine SLPHs are shown in Figs. 7 and 8, respectively. By varying solely the peak amplitude E_0 of the driving field, the harmonic order of SLPH is successively turned from 17th to 33rd, as shown in Fig. 7. On the other hand, the overall angular frequencies of these nine SLPHs in Fig. 8 are maintained within the range from 9×10^{13} to 11×10^{13} rad/s with an average of 9.64×10^{13} rad/s. This indicates that the desired order and angular frequency of SLPH can be independently manipulated through the variation of the peak amplitude E_0 and the parameter r of the driving field, respectively.

V. CONCLUSION

In summary, we have theoretically demonstrated the generation of spinning linearly polarized harmonics (SLPH) through the combination of polarization shaping with high-order harmonic generation. Two orthogonally polarized 800-nm femtosecond pulses with carefully designed relative peak amplitude are combined to generate a near-infrared (NIR) spinning linearly polarized driving field, which is then utilized in the generation of SLPH via interaction with Ar atoms.

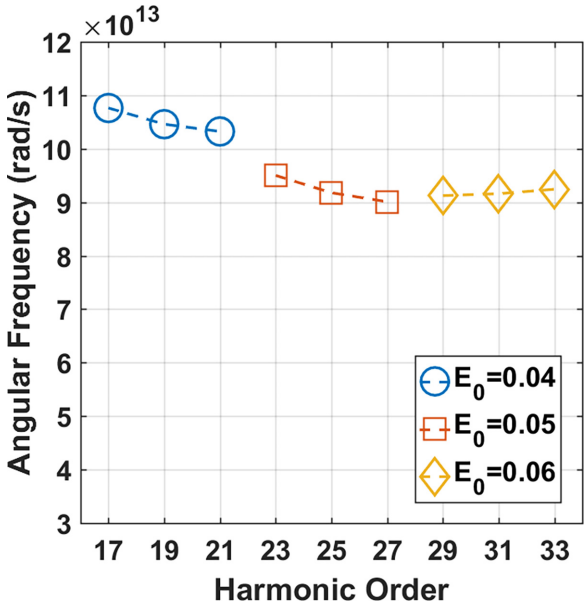

FIG. 8. The average angular frequency of SLPHs with harmonic orders from 17th to 33rd. The parameter r is fixed as 1.5, and the peak amplitude E_0 of the driving field increases from 0.04 (blue circles) to 0.05 (orange squares) and 0.06 (yellow diamonds).

The electric field of SLPH exhibit a uniformly twisted polarization with projection of a unique bow-tie shape in the X-Y plane. It is verified that by separately varying the polarization rotational speed and the peak amplitude of the driving field, the angular frequency and the harmonic order of SLPH can be manipulated independently, and this brings at least two aspects of advantages. On the one hand, these exhibited SLPHs with harmonic orders from 17th to 33rd possess a half-cycle duration on the order of several tens of attoseconds, which may lead to a temporal resolution 2 orders of magnitude higher than that achieved utilizing polarization-skewed pulses in exploring molecular dynamics [11]. On the other hand, through fine-tuning the overall range and angular frequency of the time-dependent polarization rotation of SLPH, the detection, discernment, and even control of different reaction pathways in molecules could be achieved [13]. The proposed strategy extends the photon energy of laser fields with twisted polarization into the extreme ultraviolet (EUV) region, which paves the way for the study of ultrafast dynamics on the attosecond timescale. Meanwhile, these fascinating EUV harmonics with novel polarization states may also contribute to areas such as quantum information and EUV lithography.

ACKNOWLEDGMENTS

This research was funded by the National Natural Science Foundation of China (NSFC) (Grants No. 11604119, No. 11627807, and No. 12204191) and the National Key Research and Development Program of China (Grant No. 2022YFE0134200).

[1] A. Korobenko, A. A. Milner, and V. Milner, Direct observation, study, and control of molecular superrotors, Phys. Rev. Lett. **112**, 113004 (2014).

[2] I. Tutunnikov, E. Gershnabel, S. Gold, and I. S. Averbukh, Selective orientation of chiral molecules by laser fields with twisted polarization, J. Phys. Chem. Lett. **9**, 1105 (2018).

[3] U. Steinitz, Y. Prior, and I. S. Averbukh, Laser-induced gas vortices, Phys. Rev. Lett. **109**, 033001 (2012).

[4] K. Kitano, H. Hasegawa, and Y. Ohshima, Ultrafast angular momentum orientation by linearly polarized laser fields, Phys. Rev. Lett. **103**, 223002 (2009).

[5] S. Zhdanovich, A. A. Milner, C. Bloomquist, J. Floß, I. S. Averbukh, J. W. Hepburn, and V. Milner, Control of molecular rotation with a chiral train of ultrashort pulses, Phys. Rev. Lett. **107**, 243004 (2011).

[6] J. Karczmarek, J. Wright, P. Corkum, and M. Ivanov, Optical centrifuge for molecules, Phys. Rev. Lett. **82**, 3420 (1999).

[7] G. Karras, M. Ndong, E. Hertz, D. Sugny, F. Billard, B. Lavorel, and O. Faucher, Polarization shaping for unidirectional rotational motion of molecules, Phys. Rev. Lett. **114**, 103001 (2015).

[8] O. Faucher, E. Prost, E. Hertz, F. Billard, B. Lavorel, A. A. Milner, V. A. Milner, J. Zyss, and I. S. Averbukh, Rotational Doppler effect in harmonic generation from spinning molecules, Phys. Rev. A **94**, 051402(R) (2016).

[9] E. Prost, H. Zhang, E. Hertz, F. Billard, B. Lavorel, P. Bejot, J. Zyss, I. S. Averbukh, and O. Faucher, Third-order-harmonic generation in coherently spinning molecules, Phys. Rev. A **96**, 043418 (2017).

[10] J. Bert, E. Prost, I. Tutunnikov, P. Béjot, E. Hertz, F. Billard, B. Lavorel, U. Steinitz, I. S. Averbukh, and O. Faucher, Optical imaging of coherent molecular rotors, Laser Photonics Rev. **14**, 1900344 (2020).

[11] Q. Ji, S. Pan, P. He, J. Wang, P. Lu, H. Li, X. Gong, K. Lin, W. Zhang, J. Ma, H. Li, C. Duan, P. Liu, Y. Bai, R. Li, F. He, and J. Wu, Timing dissociative ionization of H_2 using a polarization-skewed femtosecond laser pulse, Phys. Rev. Lett. **123**, 233202 (2019).

[12] S. Pan, W. Zhang, H. Li, C. Lu, W. Zhang, Q. Ji, H. Li, F. Sun, J. Qiang, F. Chen, J. Tong, L. Zhou, W. Jiang, X. Gong, P. Lu, and J. Wu, Clocking dissociative above-threshold double ionization of H_2 in a multicycle laser pulse, Phys. Rev. Lett. **126**, 063201 (2021).

[13] S. Pan, Z. Zhang, L. Xu, W. Zhang, P. Lu, Q. Ji, K. Lin, L. Zhou, C. Lu, H. Ni, C. Ruiz, K. Ueda, F. He, and J. Wu, Manipulating parallel and perpendicular multiphoton transitions in H_2 molecules, Phys. Rev. Lett. **130**, 143203 (2023).

[14] P. Eckle, M. Smolarski, P. Schlup, J. Biegert, A. Staudte, M. Schöffler, H. G. Muller, R. Dörner, and U. Keller, Attosecond angular streaking, Nat. Phys. **4**, 565 (2008).

[15] E. P. Månsson, D. Guénot, C. L. Arnold, D. Kroon, S. Kasper, J. M. Dahlström, E. Lindroth, A. S. Kheifets, A. L'Huillier, S. L. Sorensen, and M. Gisselbrecht, Double ionization probed on the attosecond timescale, Nat. Phys. **10**, 207 (2014).

[16] M. R. Hermann and J. A. Fleck, Split-operator spectral method for solving the time-dependent Schrödinger equation in spherical coordinates, Phys. Rev. A **38**, 6000 (1988).

[17] T.-F. Jiang and Shih-I. Chu, High-order harmonic generation in atomic hydrogen at 248 nm: Dipole-moment versus acceleration spectrum, Phys. Rev. A **46**, 7322 (1992).

[18] J. Wang, G. Chen, F. Guo, S. Li, J. Chen, and Y. Yang, High-intensity molecular harmonic generation without ionization, Chin. Phys. B **22**, 033203 (2013).